REPORT DOCUMENTATION PAGE

1. REPORT DATE (DD-MM-YYYY)	2. REPORT TYPE	3. DATES COVERED (From - To)
23-11-2010	Journal Article	

4. TITLE AND SUBTITLE

Decomposition Measurements of RP-1, RP-2, JP-7, n-Dodecane, and Tetrahydroquinoline in Shock Tubes (Preprint)

5a. CONTRACT NUMBER

5b. GRANT NUMBER

5c. PROGRAM ELEMENT NUMBER

6. AUTHOR(S)

Megan E. MacDonald, David F. Davidson, Ronald K. Hanson (Stanford University)

5d. PROJECT NUMBER

5f. WORK UNIT NUMBER
33SP0840

7. PERFORMING ORGANIZATION NAME(S) AND ADDRESS(ES)

Stanford University
Mechanical Engineering Department
440 Escondido Mall, Bldg 530
Stanford, CA, 94305-3030

8. PERFORMING ORGANIZATION REPORT NUMBER

AFRL-RZ-ED-JA-2010-515

9. SPONSORING / MONITORING AGENCY NAME(S) AND ADDRESS(ES)

Air Force Research Laboratory (AFMC)
AFRL/RZS
5 Pollux Drive
Edwards AFB CA 93524-7048

10. SPONSOR/MONITOR'S ACRONYM(S)

11. SPONSOR/MONITOR'S NUMBER(S)
AFRL-RZ-ED-JA-2010-515

12. DISTRIBUTION / AVAILABILITY STATEMENT

Approved for public release; distribution unlimited (PA #10611).

14. ABSTRACT

Fuel time-histories and overall rates of gas-phase RP-1, RP-2, JP-7, n-dodecane, and 1,2,3,4-tetrahydroquinoline decomposition reactions were measured using laser absorption in an aerosol shock tube and a heated high-pressure shock tube. Experiments were performed with 0.1% to 0.6% fuel/argon mixtures for temperatures between 1000 and 1400 K and pressures from 3 to 51 atm. Fuel concentration was measured by infrared laser absorption at 3.39 μm using absorption cross sections also reported here. Fuel-removal data for n-dodecane were also used to determine the unimolecular decomposition rate constant for the reaction n-dodecane → products.

15. SUBJECT TERMS

16. SECURITY CLASSIFICATION OF:			17. LIMITATION OF ABSTRACT	18. NUMBER OF PAGES	19a. NAME OF RESPONSIBLE PERSON
a. REPORT	**b. ABSTRACT**	**c. THIS PAGE**			Mr. Matthew Billingsley
Unclassified	Unclassified	Unclassified	SAR	28	**19b. TELEPHONE NUMBER** (include area code) N/A

Decomposition Measurements of RP-1, RP-2, JP-7, n-Dodecane, and Tetrahydroquinoline in Shock Tubes

Megan E. MacDonald[1], David F. Davidson[2] and Ronald K. Hanson[3]
Stanford University, Stanford, CA, 94305

Fuel time-histories and overall rates of gas-phase RP-1, RP-2, JP-7, n-dodecane, and 1,2,3,4-tetrahydroquinoline decomposition reactions were measured using laser absorption in an aerosol shock tube and a heated high-pressure shock tube. Experiments were performed with 0.1% to 0.6% fuel/argon mixtures for temperatures between 1000 and 1400 K and pressures from 3 to 51 atm. Fuel concentration was measured by infrared laser absorption at 3.39 μm using absorption cross sections also reported here. Fuel-removal data for n-dodecane were also used to determine the unimolecular decomposition rate constant for the reaction n-dodecane → products.

Nomenclature

a, b, c, d = coefficients for polynomial fits to absorption cross sections

$a_1, a_2, a_3, a_4, a_5, a_6, a_7$ = coefficients for the NASA polynomial used to calculate thermodynamic properties

I = laser intensity after passing through an absorbing medium

I_o = laser intensity before passing through an absorbing medium

I_2 = laser intensity after passing through the absorbing medium in region 2

$k_{overall}$ = decomposition rate due to all elementary reactions during initial fuel decomposition in s^{-1}

L = path length through the absorbing medium in m

N = the number density (of fuel molecules) in the test mixture in mol/m^3

P_{total} = total pressure in the shock tube in N/m^2

R = the gas constant in units of $K\text{-}m^3/atm\text{-}mol$

---

[1] Graduate Research Assistant, Mechanical Engineering, 452 Escondido Mall, Stanford University, AIAA Student Member.
[2] Senior Research Scientist, Mechanical Engineering, 452 Escondido Mall, Stanford University, AIAA Member.
[3] Professor, Mechanical Engineering, 452 Escondido Mall, Stanford University, AIAA Fellow.

T	=	temperature in K
t	=	time
X_{fuel}	=	fuel mole fraction
α_2	=	absorbance in region 2
α_5	=	absorbance in region 5
α_{meas}	=	experimentally measured absorbance
α_{prod}	=	absorbance due to the interfering product species
α_{fuel}	=	absorbance due to the fuel
$\sigma(T, \lambda)$ =		absorption cross section (function of temperature and wavelength) in m^2/mol

I. Introduction

HIGH-performance regeneratively cooled engines require fuel that not only performs well as a propellant but also acts as a coolant for the engine. Operating temperatures of the engines in these high-performance vehicles are continually increasing and are reaching the point at which research into the formation of coke (solid carbonaceous deposits) in the cooling channels, which restricts the flow and hinders the heat transfer process, has become critical. Three main mechanisms of coke formation have been described in the literature: oxidative, catalytic, and pyrolytic [1-5]. Here, the focus is on understanding the initial gas-phase kinetic processes that lead to the formation of pyrolytic coke. This coking mechanism is predominant at temperatures above 825 K and occurs when the fuel is heated enough to decompose into reactive fuel radicals, leading to the eventual formation of coke [3].

There is a need to characterize the high-temperature decomposition rates of both rocket fuels and the fuel surrogates used to simulate the kinetic behavior of these fuels. Of particular importance is the decomposition behavior of n-dodecane, a single-component n-alkane surrogate.   Overall fuel decomposition rates were identified as a useful means of observing the decomposition of fuels such as n-dodecane as early as 1939 when Tilicheev published "cracking velocity constants" for n-alkanes from C_5 to C_{32} at 150 atm and 673 to 848 K [6]. Since that time, n-dodecane decomposition rates have been measured under a variety of conditions. In 1945, Greensfelder and Voge published a "first-order thermal velocity constant" for the thermal cracking of n-dodecane as it passed through a continuous flow reactor at 773 K and atmospheric pressure [7]. In a following publication, Voge and Good reported similar measurements for n-hexadecane, listed the currently existing thermal cracking rates for n-alkanes

from C_4 to C_{16}, and proposed an empirical correlation between decomposition rate and carbon number [8]. In 1986, Zhou and Crynes reported pseudo-first-order rate constants at 623 and 673 K for the decomposition of n-dodecane in a batch reactor pressurized to 9.2 MPa (91 atm) with nitrogen or hydrogen [9]. A continuation of this work resulted in the publication of decomposition rates for n-alkanes and mixtures of n-alkanes from C_9 to C_{22} in a flowing tube reactor at atmospheric pressure and temperatures from 623 to 893 K [10]. In 1996, Yoon et al. completed micro-reactor studies of n-dodecane decomposition rates in nitrogen at pressures of 0.69 to 1 MPa (6.8 to 9.9 atm) and temperatures of 673 to 723 K [11, 12]. A subsequent publication reported additional n-dodecane decomposition rates [13]. In 2007, shock tube studies of high-temperature (1100 to 1300 K) decomposition of n-dodecane were completed in the 0.3 to 6 atm pressure range [14]. Watanabe et al. give a thorough overview of rate constants for a wide range of n-alkanes and propose a model for estimating these rates [15].

Overall fuel decomposition rates for RP-fuels and other kerosenes have also appeared in the literature. In 1984, Van Camp et al. reported rate coefficients for steam-diluted kerosene subjected to temperatures of 930 to 1100 K while flowing through a 1 cm diameter, 22 m long cell encased in a furnace. In order to report a rate for this mixture of hydrocarbons, the kerosene was considered a single "pseudo-component" and a GC-MS analysis of the kerosene sample was included in order to define its components [16]. Dworzanski et al. performed studies on pentadecane and JP-7 at atmospheric pressure and reported Arrhenius plots containing rate constants for both in the 800 to 1100 K temperature range [17]. NIST has recently published decomposition rate constants for Jet A [18], RP-1 [19, 20], and RP-2 [20, 21] from experiments carried out in ampule reactors at pressures near 34.5 MPa (340 atm) and temperatures from 648 to 773 K.

Studies of various additives intended to alter the decomposition and deposition rates of fuels have also been conducted and reported in the literature [3, 4, 11, 12, 21-25]. Of the additives tested, these studies indicate that 1,2,3,4-tetrahydroquinoline (THQ) is one of the most effective at decreasing pyrolytic deposits.

Here we report first-order overall fuel decomposition rates obtained from laser-absorption time histories for the kerosenes RP-1, RP-2, and JP-7, and the single-component chemical kinetic surrogate, n-dodecane ($C_{12}H_{26}$). Also investigated are the effects of a hydrogen-donor additive, 1,2,3,4-tetrahydroquinoline ($C_9H_{11}N$) on these fuels. It should be noted that the overall fuel decomposition rates reported here include the effects of all elementary reactions occurring within the first few milliseconds of decomposition. Examples of the use of fuel decomposition data to determine the elementary reaction rate constant for the reaction, n-dodecane → products, are also presented.

II. Theory

To determine time-histories and decomposition rates from shock tube/laser absorption measurements, two key concepts are employed: Beer's law, given as Eq. (1), and the assumption of pseudo-first-order reactions. Beer's law relates the fractional transmission of monochromatic light through an absorbing medium, $(I/I_o)_\lambda$, to the number density of absorbers:

$$(I/I_o)_\lambda = \exp(-\sigma_\lambda N L) \tag{1}$$

N can also be expressed as $N = X_{fuel} P_{total} / RT$, which enables us to relate absorbance $\alpha = -\ln(I/I_o)$ to fuel mole fraction:

$$X_{fuel}(t) = -\ln(I/I_o) RT / \sigma_\lambda P_{total} L \tag{2}$$

Each fuel has a relatively unique absorption band structure. The cross section at wavelength λ, σ_λ, in m^2/mol, is a measure of the absorption strength of the fuel vapor. It is a function of wavelength and of the temperature of the fuel vapor, but for the high molecular weight fuels in this study it is effectively independent of pressure.

The absorption cross sections of n-dodecane, RP-1, RP-2, JP-7, and THQ in gaseous form were measured in a heated cell using a Nicolet 6700 FTIR over the 3.3 to 3.6 μm wavelength region at temperatures up to 775 K. Reference [26] describes the procedure for measuring the gaseous cross sections of liquid fuel blends. The current study differed in procedure from [26] only in that here, measurements have been performed on undiluted, fully-evaporated fuels at low pressures. The low-temperature cross section of n-dodecane was reported in [27] and its high-temperature cross section was reported in [28]. (Reference [28] also reported preliminary JP-7 cross sections, which have been updated here.) Absorption cross sections as a function of wavelength for RP-1, RP-2, JP-7, and THQ are shown at two temperatures in Fig. 1; the mid-infrared HeNe laser wavelength, 3.39 μm, has been labeled for each fuel. The selection of the HeNe laser wavelength is discussed in further detail in the Section III. The heated-cell temperature-dependent cross sections of these fuels at 3.39 μm are shown in Fig. 2.
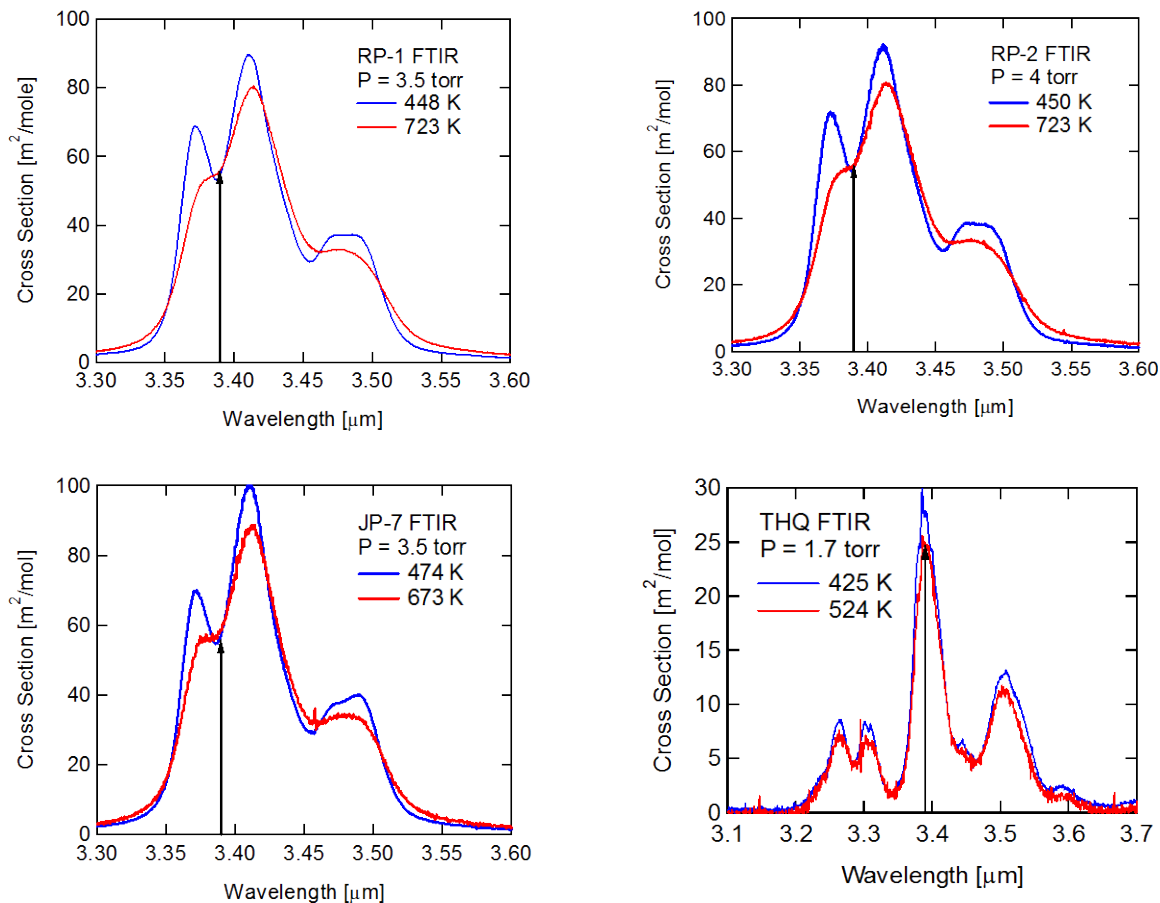
Fig. 1 Absorption cross sections of undiluted RP-1, RP-2, JP-7, and THQ measured by FTIR. The 3.39 μm wavelength of a mid-IR HeNe laser is indicated.

The measured FTIR cross sections were limited to temperatures below approximately 800 K because the fuel began to decompose in the cell faster than the measurement could be completed. To obtain high-temperature cross sections, shock wave experiments were utilized. In such an experiment, region 2 is the label given to the gas that has been shocked by only the incident shock and region 5 is the label given to the gas that has been shocked by both the incident and reflected shock waves. Fuel concentration in region 2 can be determined by using the measured absorbance behind the incident shock wave, $\alpha_2 = -\ln(I_2/I_o)$, and the FTIR cross section for T_2. The fuel cross section, σ_5, at the higher pressure and temperature of region 5, immediately behind the reflected shock wave (where the fuel mole fraction is unchanged from region 2), can be determined from the known temperature, pressure, concentration, and absorbances in regions 2 and 5 and the cross section values in region 2. With knowledge of the cross section as

a function of temperature, the transmission through the test gas mixture, and the path length through the tube, quantitative measurements of fuel concentration in the shock tube can be made.
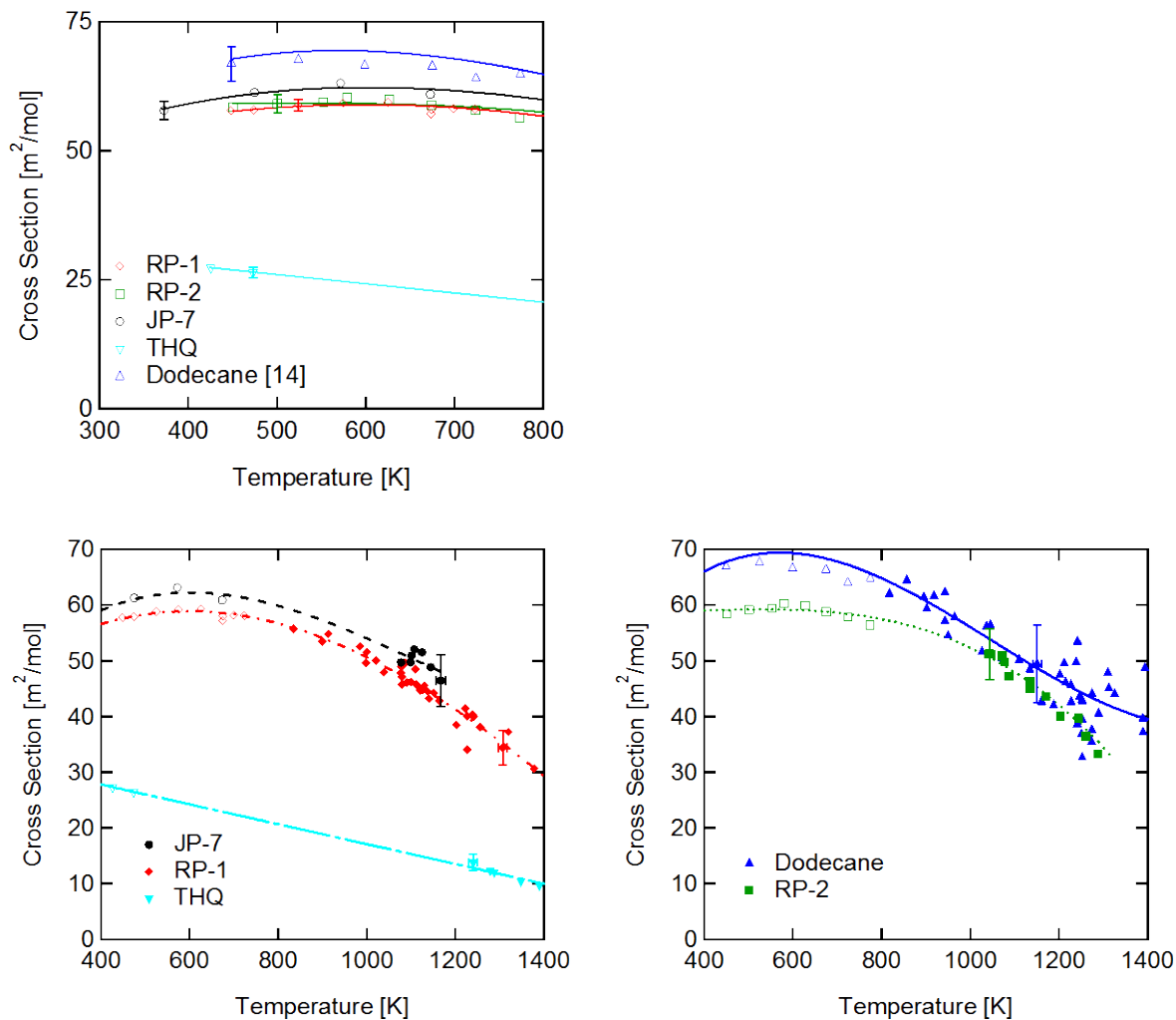

Fig. 2 Heated-cell FTIR-based absorption cross sections at 3.39 μm (300-800 K) and polynomial fits to FTIR- and shock-based absorption cross sections at 3.39 μm (400 – 1400 K).

The polynomial fits from Fig. 2 are given in Table 1, follow the form $\sigma(T) = a + b\,T + c\,T^2 + d\,T^3$, with T in K, and result in a cross section with units of m²/mol. It should be noted that these polynomials are only valid in the temperature region for which data was taken, with a lower temperature limit of 300 and an upper temperature limit of 1200 K for JP-7, 1300 K for RP-2, and 1400 K for RP-1, n-dodecane, and THQ.

Table 1 Absorption Cross Section Fits for n-Dodecane, RP-1, RP-2, JP-7, and THQ at 3.39 μm

	a	b	c	d
Dodecane	22.53	0.1884	-2.273e-4	7.244e-8
RP-1	35.94	0.08175	-8.017e-5	1.314e-8
RP-2	60.48	-0.01447	4.185e-5	-3.547e-8
JP-7	27.71	0.1311	-1.486e-4	4.397e-8
THQ	34.97	-0.01782		

The second important concept required to determine the overall fuel decomposition rate is the use of a pseudo-first-order kinetics model to describe the decomposition reactions of these fuels. Pseudo-first-order reactions follow the form shown in Eq. (3) where $k_{overall}$ is the rate of fuel removal for this decomposition reaction.

$$fuel \xrightarrow{\ k_{overall}\ } products \tag{3}$$

Solving the equation describing pseudo-first-order kinetics for the time-varying concentration or mole fraction gives:

$$X_{fuel}(t)/X_{fuel}(0) = \exp(-\ k_{overall}t) = \alpha_5(t)/\alpha_5(0) \tag{4}$$

Thus the measurements of fuel decomposition rate are actually independent of the absorption cross section for the conditions studied here.

III. Experimental Setup

Shock tubes can be used to great advantage to study the chemical kinetic behavior of fuels. A conventional shock tube is comprised of two sections, a driver and a driven section, separated by a diaphragm. The driven section is filled with a mixture of fuel and bath gas, and the driver is filled with a light gas, often helium, until the diaphragm bursts causing a shock wave to propagate down the tube into the fuel mixture, heating and pressurizing this mixture. The shock then reflects from the endwall and travels back toward the driver section, again increasing the temperature and pressure of the fuel mixture, now to the desired test conditions. Diagnostics are located at or near the endwall in order to make observations of this high-temperature, high-pressure fuel vapor. The initial fuel mixture is typically prepared manometrically in a mixing tank by sequentially filling the evacuated tank, first with

the desired partial pressure of fuel and then to the desired total pressure with bath gas. The fuel/bath gas mixture is stirred mechanically until a uniform mixture is obtained, which is then introduced into the driven section of the tube. Filling the tank with fuel is a straightforward process when the fuel is a gas at room temperature, and even liquid fuels can be introduced into the mixing tank as vapor without difficulty if their room-temperature vapor pressures are high enough. However, this vapor-pressure fill method is difficult to carry out for low-vapor-pressure fuels. In such cases, heating the fuel, mixing tank, and shock tube can extend the range of a shock tube to include studies of slightly heavier fuels. To study extremely heavy fuels with vapor pressures that are low even when the fuel, mixing tank, and shock tube are heated, an aerosol shock tube is necessary [29].

Dodecane and kerosene fuels such as RP-fuels and JP-7 lie in a region of overlap where both aerosol and heated shock tube methods can be used as complementary measurement tools. Hence, the low-pressure (< 8 atm) experiments were performed in the Second-Generation Aerosol Shock Tube (AST) facility in the High Temperature Gasdynamics Laboratory at Stanford University. The AST is an ideal method for measurement of high-carbon-number, multi-component (distilled) fuels for two major reasons. First, the fuel mole fractions that can be obtained in the AST are much higher than those obtained in a conventional shock tube. For conventional gas-phase shock tube studies, the maximum fuel mole fraction is limited by the vapor pressure of the fuel. This makes mid-infrared studies of low-vapor-pressure fuels difficult because unless the shock tube is heated, only very low concentrations of fuel can be loaded into the shock tube, and as a result, absorption is frequently too small to make accurate, quantitative measurements. The second major advantage of the AST comes as a result of its unique fuel introduction method. The fuel is nebulized into an aerosol, which is carried into the shock tube by a bath gas, therefore delivering all components of a distillate fuel into the shock tube and maintaining the original ratios of components from that distilled fuel. For a multi-component fuel, the vapor-pressure fill method could lead to a re-distillation of the fuel, leaving the heaviest components in the mixing tank. This can be avoided in certain cases by careful and proper use of a heated shock tube, but the aerosol method offers greater certainty that the ratio of components in a distilled fuel is preserved.
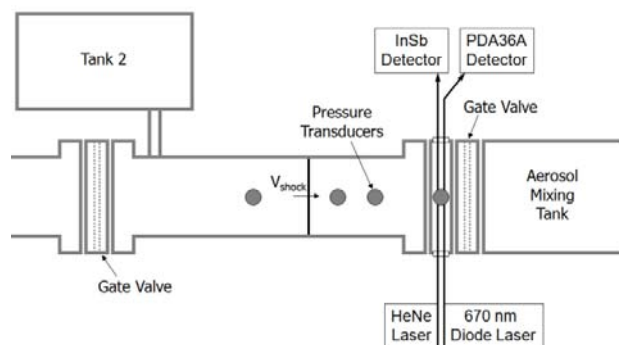
Fig. 3 Aerosol Shock Tube Setup.

The operation of the AST is slightly different than that of a conventional shock tube. An aerosol is generated in an aerosol mixing tank and then introduced into the driven section of the tube through an endwall gate valve. The incident shock vaporizes this aerosol leaving behind a uniform fuel vapor that is subsequently heated and pressurized to the desired conditions by the reflected shock. Absorption and extinction measurements are recorded at a window located 4 cm from the endwall across a path length of 10 cm. Further details concerning the aerosol delivery method are given in [28-33].

Two lasers were employed for these experiments.   The Jodon HN-10GIR is a fixed-wavelength mid-infrared HeNe gas laser operating at 3.39 μm (2947.909 cm^{-1}), a wavelength that is strongly absorbed by all of the fuels studied; see Fig. 1. However, the mid-infrared HeNe is sensitive to both aerosol scattering and vapor absorption. To confirm that the aerosol is completely vaporized during an experiment, a second, non-resonant, wavelength is employed. This non-resonant wavelength is located away from any absorption features of the fuels, intermediate species, and products and is therefore attenuated only by droplet (Mie) scattering. When the aerosol is completely vaporized, the extinction at this wavelength drops to zero indicating that the HeNe absorption is entirely due to vapor and can therefore be used to calculate the post-shock temperature and fuel mole fraction. The non-resonant wavelength (670 or 1335 nm) was generated using a diode laser. Figure 3 shows the laser layout for the AST experiments.

Because the AST was not designed to withstand high test pressures, high-pressure (> 23 atm) RP-1 and n-dodecane experiments were carried out in the High-Pressure Shock Tube (HPST) facility at Stanford University. The HPST is not equipped with an aerosol delivery system, but is equipped with a system for heating both the tube and mixing tank. In order to ensure that all components of RP-1 were completely evaporating in the mixing tank, a

simple experiment was carried out. Various amounts of fuel were injected into the mixing tank (heated to 110°C) in liquid form and then allowed to evaporate and mix for 10 minutes. It was observed that for small amounts of injected fuel, the resulting pressure in the mixing tank increased nearly linearly with amount of fuel injected. In this linear region, there was so little fuel in the tank that all components completely evaporated. This was observed to be the case up to about 2 mL of injected fuel, at which point the mixing tank pressure began rolling off to a plateau. This plateau can be observed in Fig. 4 for both RP-1 and n-dodecane and corresponds to the vapor pressure of each fuel. For dodecane at 110°C, this is 23.7 torr. As a distilled fuel consisting of hundreds of components, it is difficult to define a unique vapor pressure for RP-1. However, extrapolating the limited RP-1 vapor pressure data in [34] up to 110°C gives a "calculated vapor pressure based on initial boiling point" of 44 torr.
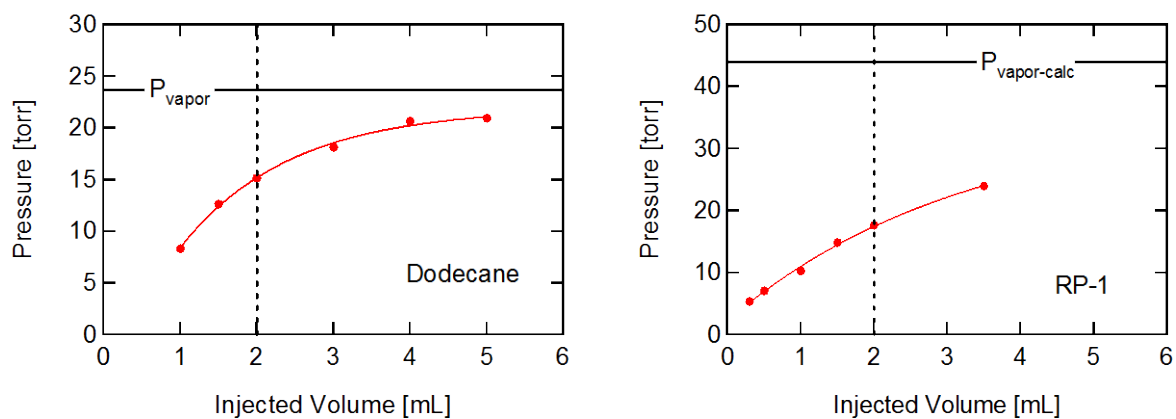

Fig. 4 HPST mixing tank complete evaporation checks. Tank temperature 110°C, tank volume 12.84 L. Solid -curves are exponential fits to the data. Significant roll-off is indicated by the dashed line and begins at 2 mL for both fuels.

This roll-off was an indication that the heaviest components of RP-1 were no longer evaporating. As long as the amount of fuel injected was below the point at which significant roll-off occurred, complete evaporation could be assumed. In the present study, to be on the conservative side of the roll-off point, the maximum RP-1 volume injected into the mixing tank was 1 mL. Argon was then added up to the desired total pressure and the mixture was stirred in the tank for one to two hours. This was found to be the ideal balance between a long mixing time required to ensure complete evaporation of heavy components and a short mixing time required to avoid fuel decomposition. Once it was certain that complete evaporation was occurring in the mixing tank, attention was turned to the shock tube itself. Because of the low room-temperature vapor pressures of the fuels tested, the entire shock tube driven

section and transfer lines were heated to 90°C in order to accommodate enough fuel in the gas phase to make absorption measurements. Since the mole fraction is constant between the mixing tank and the shock tube, and the shock tube total pressure is much lower than the mixing tank total pressure, the partial pressure of fuel is also much lower in the shock tube. This means that a lower temperature, and vapor pressure, is acceptable for the shock tube, and the fuel partial pressure can still be maintained well below its vapor pressure. The partial pressures of dodecane loaded into the shock tube varied from 5.2 to 7.6 torr, below the 9.4 torr vapor pressure of dodecane at 90°C. Taking into account the typical region 1 pressure (2 atm), the resulting n-dodecane mole fraction in the case of the smallest fuel loading was 0.3% fuel, well above the minimum detection limit at the conditions of these experiments. The minimum detectable amount of fuel (with SNR of 1) at the conditions of this study is 0.01% fuel for dodecane and 0.02% fuel for RP-1. The fuel mole fraction was measured in the shock tube just prior to the shock using 3.39 μm laser absorption with the cross section calculated from the fits given in Table 1 and the measured temperature in region 1. The mole fraction calculated from the fuel and total pressures in the mixing tank was always within 10% of the absorption-measured mole fraction. Because only vapor was present in the high-pressure shock tube studies, a HeNe laser was sufficient for these experiments (i.e., no non-resonant laser was needed). The high-pressure shock tube has a circular cross section, with an inner diameter of 5.0 cm and windows located 1.0 cm from the endwall. A detailed description of this shock tube can be found in [35, 36]. Figure 5 shows the setup for the HPST experiments.
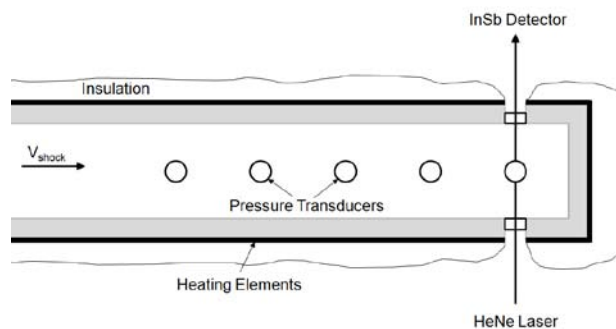

Fig. 5 High-Pressure Shock Tube Schematic.

99+% anhydrous n-dodecane and 98% 1,2,3,4-tetrahydroquinoline were obtained from Sigma-Aldrich and used as received. The JP-7 sample (POSF 3327) was obtained from the Air Force Research Laboratory (Wright-Patterson Air Force Base) while the RP-1 (lot number SH2421LS05) and RP-2 (lot number WC0721HW01) were obtained from the Air Force Research Laboratory (Edwards Air Force Base). All blended fuels were refrigerated prior to use.

The properties of JP-7, RP-1, and RP-2 are all dictated by military specification ([37] for RP-1 and RP-2, [38] for JP-7), but these specifications limit mainly chemical and physical properties, and for analysis of shock tube experiments, knowledge of the thermodynamic properties of the fuels is required. The fuel thermodynamic properties are used to calculate the ratio of specific heats for the fuel mixture. This ratio plays a key role in determining the temperature and pressure after both the incident and reflected shocks. These conditions are calculated with an in-house code called FROSH (for the HPST) that solves the normal shock jump equations. A similar, but significantly modified version called AEROFROSH is employed for the AST, and this version also requires the specific heat and enthalpy of a fuel in order to iteratively determine the post-shock temperature, pressure, and fuel mole fraction. AEROFROSH is described in more detail in [28]. The REFPROP database, which includes a surrogate mixture for the thermophysical properties of RP-1 [39], was employed to provide thermodynamic properties for RP-1. The specific heat capacity determined from the resulting NASA polynomial fits (shown in Table 2) was compared to historical data [34, 40] and agreed quite well considering the variable nature of the composition of RP-1 [41, 42]. The transition from the low- to the high-temperature polynomial was made at 475 K.

Table 2 7-Coefficient NASA polynomials for RP-1

	Low Temperature	*High Temperature*
a_1	2.22655300E+01	-2.73270218E+01
a_2	-3.17395800E-04	2.35031125E-01
a_3	3.09829900E-04	-2.25678615E-04
a_4	-5.21069400E-07	1.13132066E-07
a_5	3.34905300E-10	-2.31358409E-11
a_6	-1.66350000E+04	-1.68000000E+03
a_7	-1.57750000E+02	8.90800000E+01

It was assumed during data analysis that RP-2 and JP-7 have identical thermodynamic properties to RP-1. The low-temperature thermodynamic properties of THQ were obtained from [43] while the high-temperature properties were assumed to be equivalent to the chemically similar molecule naphthalene, which is listed in [44]. The n-dodecane thermodynamic properties were taken directly from [44].

IV.   Results and Discussion: Overall Fuel Decomposition Rates

Figure 6a shows a sample data trace for an RP-2 shock performed in the AST. Region 1 shows a constant 670 nm extinction due entirely to Mie scattering of aerosol and a constant 3.39 µm signal due to both absorption from

RP-2 and Mie scattering. The initial Schlieren spike indicates the arrival of the incident shock, after which the aerosol evaporates completely as evidenced when the 670 nm extinction drops to zero in region 2. At this point, just before the second Schlieren spike (indicating the arrival of the reflected shock), the 3.39 µm signal is due entirely to RP-2 absorption. The reflected shock raises the temperature and pressure of the test mixture to the desired conditions, and in region 5, the gradual decrease in 3.39 µm absorbance is due to the decomposition of RP-2.
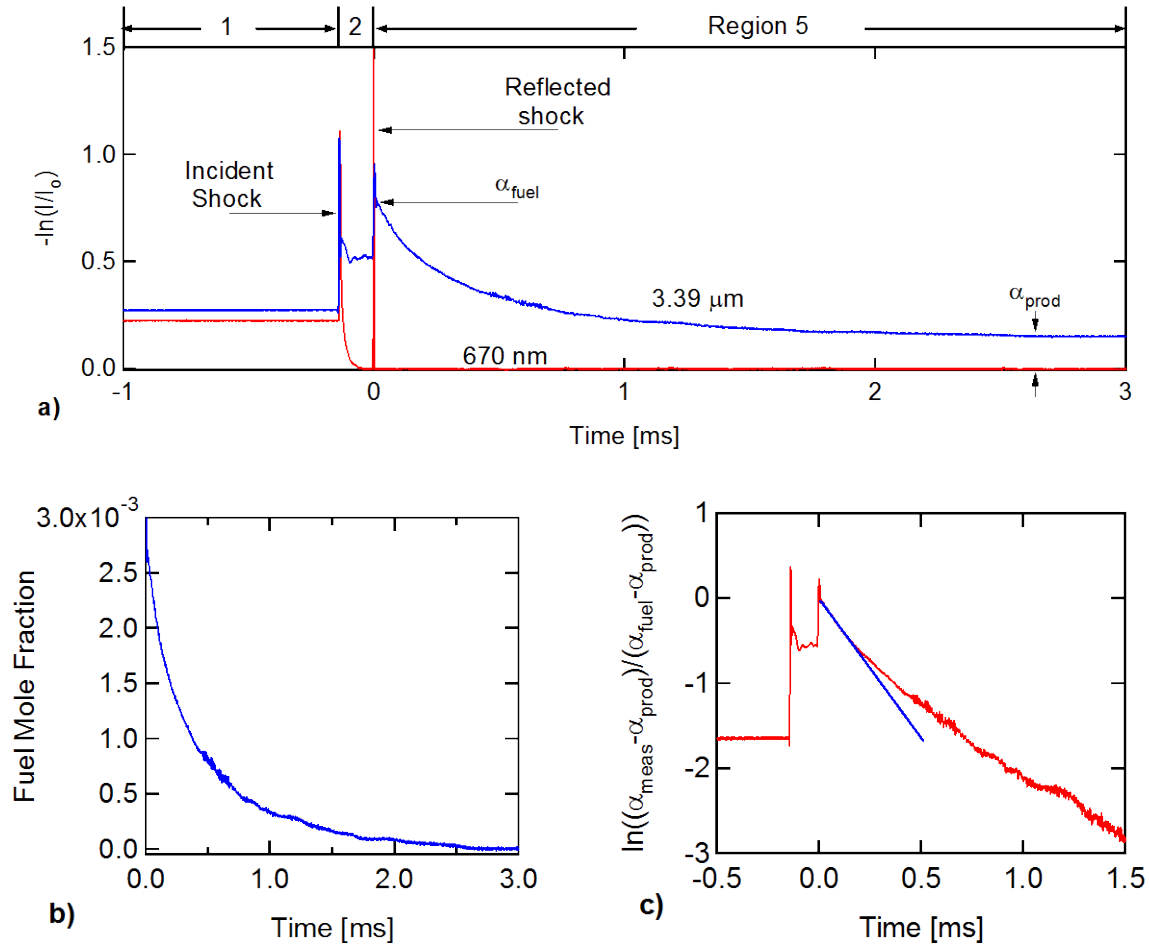

Fig. 6 a) Sample data for an RP-2 shock with 0.28% fuel concentration in argon: $V_{shock} = 740$ m/s, $P_1 = 0.29$ atm, $T_1 = 297$ K, $P_5 = 7.1$ atm, $T_5 = 1215$ K. Regions 1, 2, and 5 have been labeled. b) Fuel mole fraction time-history for the shock in a). c) Linear fit of corrected absorbance to Eq. (6), t = 0 ms corresponds to the arrival of the reflected shock.

As is obvious in Fig. 6a, at long times the HeNe wavelength is absorbed not only by the fuel, but also by decomposition products. The long-time absorbance due to products can be used to correct the time-history such that

it reflects only absorbance due to the fuel. According to the simple model given by Eq. (3), the rate of removal of fuel is equivalent to the rate of production of products. With this observation and the ideal gas assumption, the fuel mole fraction (corrected for interfering product species) can be determined from Eq. (5).
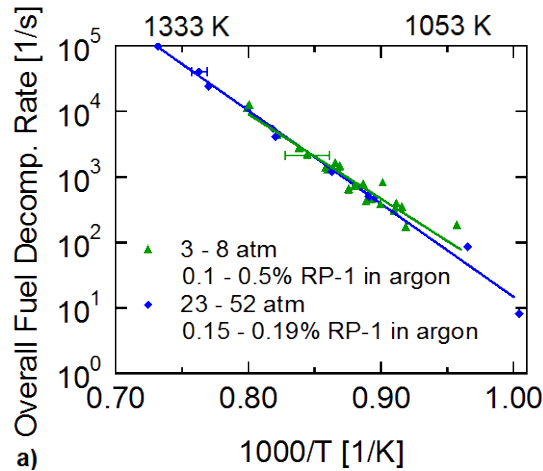
$$\frac{X_{fuel}(t)}{X_{fuel}(0)} = \frac{[\alpha_{meas}(t) - \alpha_{prod}]}{[\alpha_{fuel} - \alpha_{prod}]} \tag{5}$$

In this manner, the RP-1 mole fraction in Fig. 6b was determined from the data in Fig. 6a. Examining Eq. (4) in light of Eq. (5) results in Eq. (6), the initial slope of which, when plotted versus time (Fig. 6c), is $k_{overall}$.

$$-k_{overall}t = ln\left(\frac{\alpha_{meas}(t) - \alpha_{prod}}{\alpha_{fuel} - \alpha_{prod}}\right) \tag{6}$$

Figure 6c shows the initial first-order behavior of RP-2 decomposition, but also shows the extent of the deviation from first-order behavior as time increases beyond 0.3 ms.

The measured overall fuel decomposition rate for RP-1 from both shock tubes is shown in Fig. 7a, with the AST data in the 3-8 atm pressure range and the HPST data in the 23-52 atm pressure range. Similar n-dodecane data are shown in Fig. 7b.
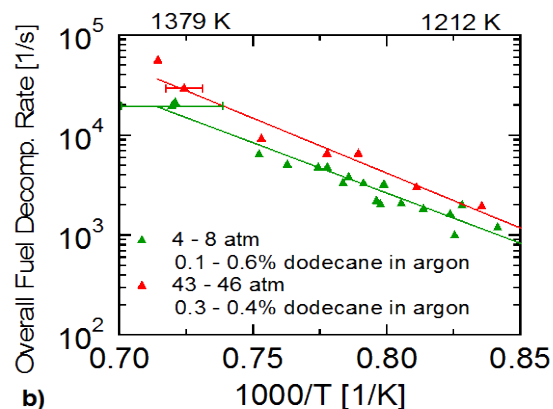

a)

Fig. 7 Comparison of overall fuel decomposition rates for low- and high-pressure RP-1 experiments and low- and high-pressure n-dodecane experiments. Solid lines are linear fits to data.

It is apparent here that there is no significant pressure dependence of this overall fuel decomposition rate for RP-1, while for n-dodecane, the overall fuel decomposition rate approximately doubles for an order of magnitude increase in pressure. This was expected, since [45] indicated that for alkanes, "the rate constant may double as the pressure is increased from 1 to 50-100 atm". Reference [46] reported no pressure dependence for measured n-hexadecane first-order rate constants in the range 14 to 68 atm, and [47] reported only a slight increase in first-order rate constant with increasing pressure for fuel mixtures containing predominately alkanes. It is expected that the predominant pathways of dodecane decomposition are the unimolecular decomposition and H-abstraction pathways. For a unimolecular reaction near the high-pressure limit, the decomposition rate does not vary with pressure; H-abstraction reactions are also independent of pressure.   Therefore, the observation of only a small pressure dependence for dodecane indicates that the decomposition rate constant is relatively close to the high-pressure limit for n-dodecane, and even closer to the limit for RP-1. The hypothesis concerning the main decomposition pathways will be examined more fully in the case of n-dodecane in the Determination of Unimolecular Decomposition Rate for n-Dodecane section, with the aid of a detailed kinetic mechanism.

No variation of the RP-1 overall fuel decomposition rate is seen with concentration over the mole fraction range of 0.1 to 0.5% fuel. In the case of n-dodecane from 4-8 atm (Fig. 7b), where no significant pressure dependence is expected, no variation in overall fuel decomposition rate is seen with concentration (which varies from 0.1 to 0.6% fuel).

The observation of a concentration-independent and nearly pressure-independent overall fuel decomposition rate allows comparison of data from both shock tubes on the same plot. The measured overall fuel decomposition rates for all of the fuels included in this study are plotted in Fig. 8. Immediately apparent is the similarity in RP-1 and RP-2 overall fuel decomposition rates. This was also found to be the case at the lower temperatures studied in [20]. Apparent, too, is that both RP-fuels decompose faster than n-dodecane in this temperature range, while the JP-7 overall fuel decomposition rates are quite similar to those of n-dodecane. THQ decomposes slightly slower than n-dodecane.
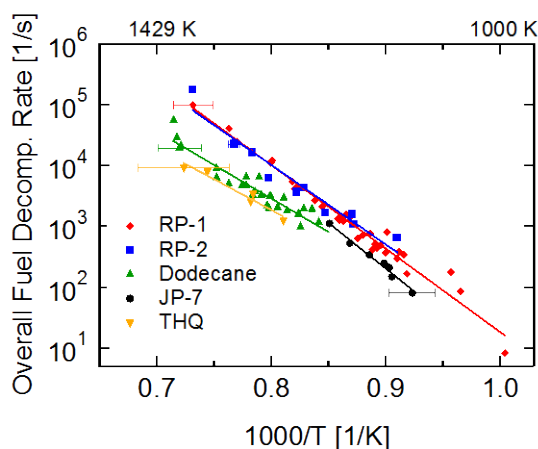

Fig. 8 Overall fuel decomposition rates for RP-1, RP-2, JP-7, 1,2,3,4-Tetrahydroquinoline, and n-dodecane. Pressure range 4 to 51 atm, 0.1 to 0.6% fuel in argon.

Given that n-dodecane has often been considered as a single-component surrogate for kerosene oxidation, and its carbon number and molecular formula are similar to those approximated for RP-fuels, the question arises as to why the overall fuel decomposition rates for n-dodecane are slower than for RP-fuels. RP-fuels are clearly more reactive than n-dodecane, and this higher reactivity must be related to the influence of components other than n-alkanes that are found in RP-fuels. References [42, 48] indicate that RP-1 actually contains a large fraction of iso-alkanes, and these are known to have faster decomposition rates than n-alkanes [49]. This observation suggests that an RP-fuel surrogate may also need to include a more reactive (i.e. more rapidly decomposing) component such as a branched alkane, if it is to successfully match the overall fuel decomposition rate of RP-fuel.

The activation energy, i.e. slope of the fit to the data in an Arrhenius plot, has been measured for each of the fuels in Fig. 8 and is listed in Table 3 and compared to values found in the literature.

Table 3 Activation Energies

Fuel	E_a [converted to kJ/mol]	Temperature Range [converted to K]	Pressure Range [converted to atm]	Reference
n-Dodecane	213 +/- 15	1110 – 1500	4 – 46	Current study
	268	1100 – 1300	0.3 – 6	14
	260 +/- 8	673 – 723	9.9 – 99	13
	264	673 – 723		50
	242	673 – 733	6.8	12
	164	623 – 893	1	10
	273	523 – 713	91	9
	234	823 – 953	1	51
	251	673 – 773	150	6
RP-1	263 +/- 7	1000 – 1370	4 – 51	Current study
	201 +/- 39	648 – 723	340	20
	87 +/- 15[a]	648 – 773	340	19
RP-2	250 +/- 23	1050 – 1370	6.4 – 7.6	Current study
	180 +/- 30	648 – 723	340	20
JP-7	287 +/- 19	1080 – 1180	4.5 – 5.2	Current study
	157	623 – 1200	102	17
Jet A	220 +/- 10	648 – 723	340	18
Kerosene	168	873 – 1123	1	16
THQ	193 +/- 26	1230 – 1380	4.3 – 4.7	Current study

a. The analysis of this sample of RP-1 showed that it was out of specification for high olefin content.

Figure 9 compares the first-order decomposition rates from this study for various kerosenes (RP-1, RP-2, and JP-7) to those found in the literature; Fig. 10 is a similar comparison of n-dodecane rates. It should be noted that the rates shown for [16] are only for the non-aromatic fraction of the kerosene studied. Their kerosene was described as "light aromatic and naphthenic," so neglecting the influence of aromatics on the decomposition rate could account for the low activation energy as compared to the other data in Fig. 9. As can be seen in Fig. 9 and Fig. 10, all previous experiments, with the exception of [14], were completed at lower temperatures than the current study. The solid line in Fig. 9 is an Arrhenius fit to all of the RP-1 and RP-2 data shown in the figure. The difference in the fits to the RP-1 and RP-2 data sets over ten orders of magnitude was negligible. Therefore a single fit was made to all RP-fuels, and it follows the form $k = A \exp(-E_a/RT)$. The resulting pre-exponential factor for RP-fuels is 3.33×10^{13} s^{-1} and the activation energy obtained from this fit is 230 kJ/mol. Similarly, the solid line in Fig. 10 is a fit to all of the dodecane data shown, and the resulting pre-exponential factor and activation energy for dodecane are 7.46×10^{12} s^{-1} and 227 kJ/mol, respectively.
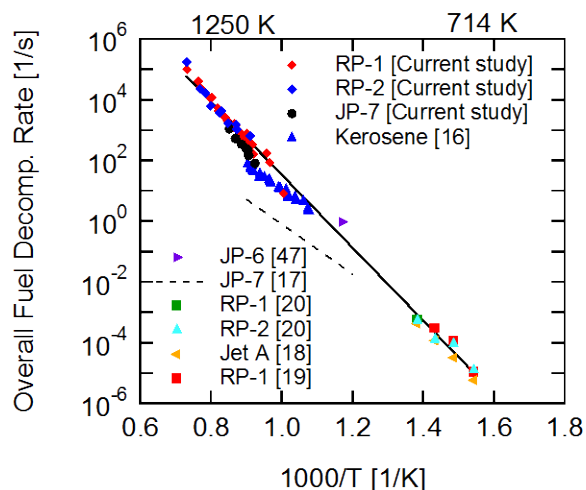
Fig. 9 Overall fuel decomposition rates for various kerosenes. Current study: 4 - 51 atm, 0.1 - 0.6% fuel in argon. Solid line is a fit to all RP-fuel data.
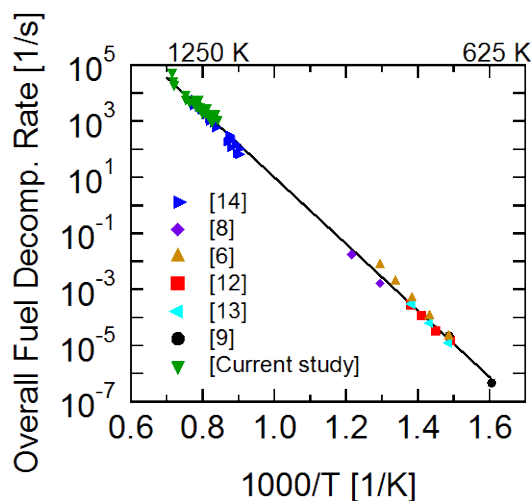

Fig. 10   Overall fuel decomposition rates for n-dodecane. Current study: 4 - 46 atm, 0.1 - 0.6% fuel in argon. Solid line is a fit to all n-dodecane data.

Figure 11 shows the effect of the additive THQ on both RP-1 and dodecane overall fuel decomposition rates.   At the lower temperatures studied by [12] (not shown), the addition of 10 mol % THQ lowers the decomposition rate significantly (about 95% at 400°C and 85% at 450°C). However, at the temperatures studied here (1150-1400K), the addition of up to 10% THQ by volume (17 mol %) has no impact on the n-dodecane overall fuel decomposition rate.   This confirms a trend observed in the low-temperature study: THQ has a decreasing effectiveness as

temperature is increased. It is suspected that this is due to high-temperature decomposition of THQ, which itself decomposes before it can act as a hydrogen donor to slow decomposition of the fuel.
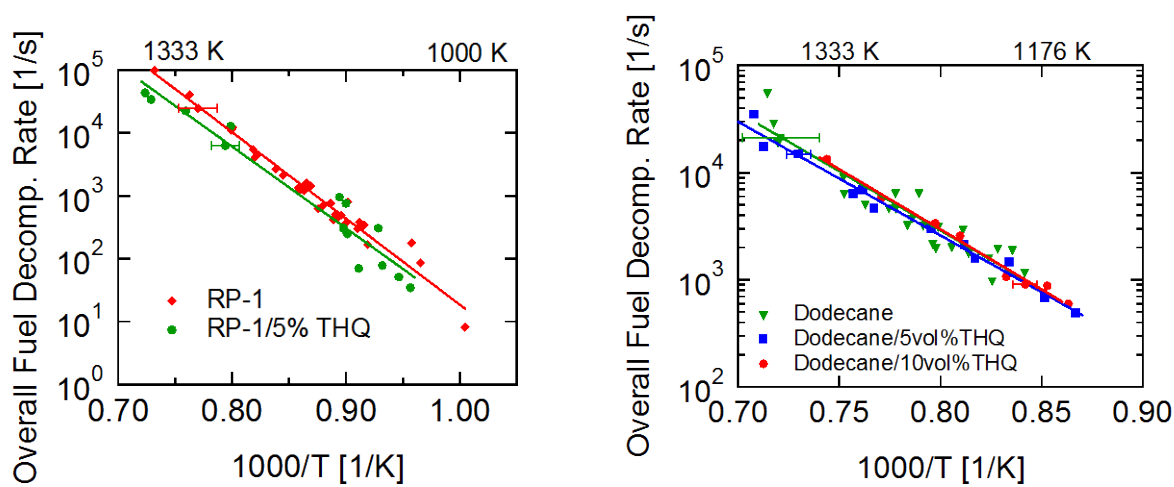

Fig. 11   **Effects of THQ on overall fuel decomposition rates. RP-1: 3 - 51 atm, 0.1 - 0.6% fuel in argon. n-Dodecane: 4 - 46 atm, 0.1 - 0.6% fuel in argon. Solid lines are fits to data.**

V.   Determination of Unimolecular Decomposition Rate for n-Dodecane

In addition to overall fuel decomposition rates, unimolecular decomposition rate constants for n-dodecane can be extracted from the data taken in these experiments. Here the term unimolecular decomposition rate constant is the rate constant, k_1, for the reaction n-dodecane → products. This rate constant is determined by fitting simulated fuel mole fraction profiles, obtained from a detailed kinetic mechanism, to measured n-dodecane profiles by varying k_1. The ratios between the rate constants for all n-dodecane decomposition channels were those from the JetSurF 1.0 mechanism [52] and were maintained in the fitting process. Although the measured overall fuel decomposition rates include effects of n-dodecane removal through both the H-abstraction and unimolecular decomposition pathways, the argument is made here that only by adjusting the unimolecular rate constants will any change in the overall fuel decomposition rate be observed. The unimolecular rate constant is determined for only dodecane. In order to complete a similar analysis for the distilled fuels, a chemical kinetic surrogate mixture would need to be selected to represent each fuel in simulations, and although this task is an important following step to the work completed here, it is beyond the scope of the current paper.

Predictions of unimolecular decomposition rates for n-dodecane were calculated using the JetSurF 1.0 mechanism and the chemical kinetic solver software CHEMKIN-PRO to gain insight as to what might be the

primary reaction pathways of this decomposition process. Other mechanisms also exist that include n-dodecane chemistry, many of them designed specifically to model jet fuel oxidation [53-57]. Both rate of production, $d[C_{12}H_{26}]/dt$, and sensitivity analyses, with a normalized sensitivity coefficient defined as $S_i = (d[C_{12}H_{26}]/dk_i)(k_i/[C_{12}H_{26}])$, were conducted. According to rate of production simulations using JetSurF 1.0, although the fastest method of n-dodecane removal is through the H-abstraction process, and unimolecular decomposition is only a secondary removal method (see Fig. 12a), the H-abstraction reaction rates are so fast that the n-dodecane profiles are quite insensitive to reasonable changes in these rates (see Fig. 12b). It follows that the overall fuel decomposition rate of n-dodecane is controlled primarily by the rate of the unimolecular decomposition process.
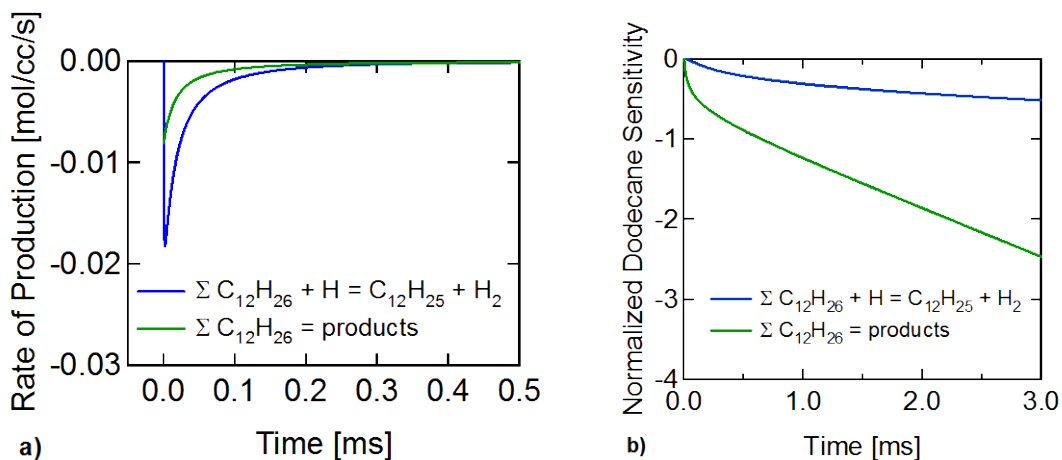

Fig. 12   **a) Rate of production and b) Sensitivity plots for JetSurF 1.0 predictions given the conditions 1286 K, 44.1 atm, and 0.33% n-dodecane in argon.**

By adjusting the rate coefficients for the unimolecular decomposition reactions in the JetSurF 1.0 mechanism, agreement can be obtained between the model-predicted n-dodecane time history and that measured in shock tube experiments. High- and low-pressure examples are shown in Fig. 13.
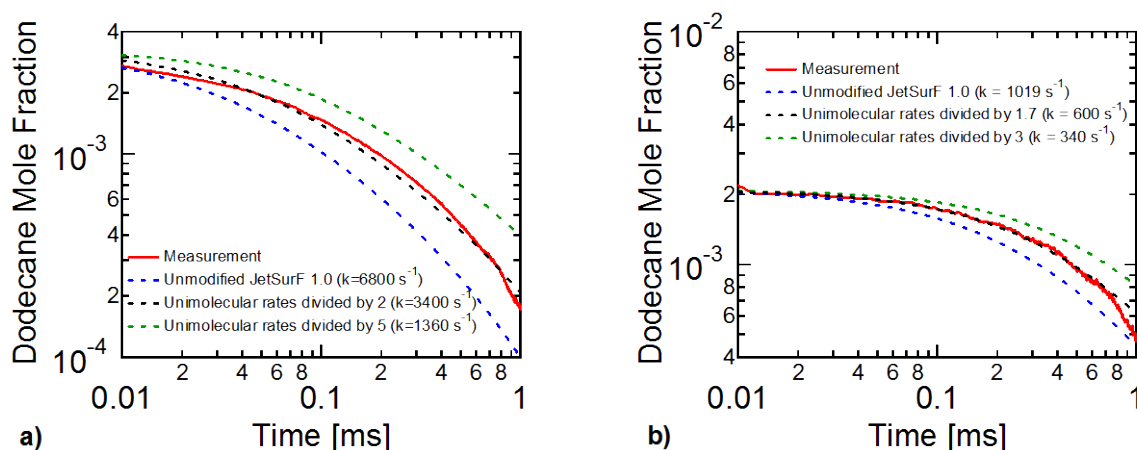
Fig.13 JetSurF 1.0 prediction of n-dodecane mole fraction at a) 1286 K, 44.1 atm, and 0.33% n-dodecane in argon. b) 1214 K, 4.7 atm, and 0.21% n-dodecane in argon.

From Fig. 13 it is observed that the JetSurF 1.0 n-dodecane unimolecular decomposition rate constants are approximately two times faster than required for a best fit to the data for two temperatures near 1250 K and pressures from 4.7 to 44.1 atm. At 1286 K and 44.1 atm, the best-fit unimolecular decomposition rate constant is 3400 s^{-1}, while at 1214 K and 4.7 atm, it is 600 s^{-1}.

VI. Conclusion

From the current data, it can be concluded that in the temperature range 1000 K to 1400 K, RP-1 and RP-2 have nearly identical overall fuel decomposition rates, n-dodecane and JP-7 both decompose slower than RP-fuels, and that the addition of THQ has a negligible effect on the overall fuel decomposition rates of both RP-1 and n-dodecane. The AST has proven to be a useful tool for measuring species time-histories and overall fuel decomposition rates of heavy and multi-component fuels and for determining the effect of the additive THQ on overall fuel decomposition rates. Fuel decomposition rates derived from measurements in the AST agreed well with rates derived in the HPST leading to the conclusion that these overall fuel decomposition rates are independent of pressure for RP-1 and that the overall fuel decomposition rates for n-dodecane approximately double with an order of magnitude increase in pressure.

Acknowledgments

References

[1]   Albright, L.F., and Marek, J.C., "Mechanistic Model for Formation of Coke in Pyrolysis Units Producing   Ethylene" *Industrial and Engineering Chemistry Research*, Vol. 27, No. 5, 1988, pp. 755-759.
      doi: 10.1021/ie00077a006

[2]   Nohara, D., Sakai, T., "Kinetic Study of Model Reactions in the Gas Phase at the Early Stages of Coke Formation," *Industrial and Engineering Chemistry Research*, Vol. 31, No. 1, 1992, pp. 14-19.
      doi: 10.1021/ie00001a003

[3]   Wickham, D.T., Atria, J.V., Engel, J.R., Hitch, B.D., Karpuk, M.E., and Striebich, R., "Formation of Carbonaceous Deposits in a Model Jet Fuel under Pyrolysis Conditions" *Symposium on Structure of Jet Fuels V*, Preprints of the American Chemical Society, Division of Petroleum Chemistry, Boston, MA, Vol. 43, 1998, pp. 428-432.

[4]   Minus, D.K., Corporan, E., "Thermal Stabilizing Tendencies of Hydrogen Donor Compounds in JP-8+100 Fuel," *35th AIAA/ASME/SAE/ASEE Joint Propulsion Conference*, Los Angeles, CA, AIAA Paper 99-2214, June 1999.

[5]   Edwards, T., "Cracking and Deposition Behavior of Supercritical Hydrocarbon Aviation Fuels," *Combustion Science and Technology*, Vol. 178, No. 1, 2006, pp. 307-334.
      doi: 10.1080/00102200500294346

[6]   Tilicheev, M.D., "Kinetics of Cracking of Hydrocarbons Under Pressure. First article. Cracking normal paraffin hydrocarbons," *Foreign Petroleum Technology*, Vol. 7, No. 5/6, 1939, pp. 209-224.

[7]   Greensfelder, B.S., Voge, H.H., "Catalytic cracking of pure hydrocarbons," *Industrial and Engineering Chemistry*, Vol. 37, No. 6, 1945, pp. 514-520.
      doi: 10.1021/ie50426a008

[8]   Voge, H.H., Good, G.M., "Thermal Cracking of Higher Paraffins," *Journal of the American Chemical Society*, Vol. 71, No. 2, 1949, pp. 593-597.
        doi: 10.1021/ja01170a059

[9]   Zhou, P., Crynes, B.L., "Thermolytic Reactions of n-dodecane," *Industrial and Engineering Chemistry Process Design and Development*, Vol. 25, No. 2, 1986, pp. 508-514.
        doi: 10.1021/i200033a027

[10] Zhou, P., Hollis, O.L., Crynes, B.L., "Thermolysis of Higher Molecular Weight Straight-Chain Alkanes (C9-C22)," *Industrial and Engineering Chemistry Research*, Vol. 26, No. 4, 1987, pp. 846-852.

doi: 10.1021/ie00064a038

[11] Yoon, E.M., Selvaraj, L., Eser, S., and Coleman, M., "High-Temperature Stabilizers for Jet Fuels and Similar Hydrocarbon Mixtures. 1. Comparative Studies of Hydrogen Donors," *Energy & Fuels*, Vol. 10, No. 3, 1996, pp. 806-811.

doi: 10.1021/ef950228l

[12] Yoon, E.M., Selvaraj, L., Eser, S., and Coleman, M., "High-Temperature Stabilizers for Jet Fuels and Similar Hydrocarbon Mixtures. 2. Kinetic Studies," *Energy & Fuels*, Vol. 10, No. 3, 1996, pp. 812-815.

doi: 10.1021/ef950229d

[13] Yu, J., Eser, S., "Kinetics of Supercritical-Phase Thermal Decomposition of C10-C14 Normal Alkanes and Their Mixtures," *Industrial and Engineering Chemistry Research*, Vol. 36, No. 3, 1997, pp. 585-591.

doi: 10.1021/ie9603934

[14] Klingbeil, A.E., Jeffries, J.B., Davidson, D.F., Hanson, R.K., "Two-Wavelength Mid-IR Diagnostic for Temperature and n-Dodecane Concentration in an Aerosol Shock Tube," *Applied Physics B*, Vol. 93, No. 2-3, 2008, pp. 627-638.

doi: 10.1007/s00340-008-3190-4

[15] Watanabe, M., Adschiri, T., Arai, K., "Overall Rate Constant of Pyrolysis of n-Alkanes at a Low Conversion Level," *Industrial and Engineering Chemistry Research*, Vol. 40, No. 9, 2001, pp. 2027-2036.

doi: 10.1021/ie000796a

[16] Van Camp, C.E., Van Damme, P.S., Froment, G.F, "Thermal Cracking of Kerosene," *Industrial and Engineering Chemistry Process Design and Development*, Vol. 23, No. 1, 1984, pp. 155-162.

doi: 10.1021/i200024a026

[17] Dworzanski, J.P., Chapman, J.N., Meuzelaar, H.L.C., Lander, H.R., "Development of Microscale Reactors Directly Interfaced to GC/IR/MS Analytical System for High Temperature Pyrolytic Degradation Studies of Jet Fuels in the Gas Phase or Under Supercritical Conditions," *Symposium on Structure of Jet Fuels III*, Preprints of the American Chemical Society, Division of Petroleum Chemistry, San Francisco, CA, Vol. 37, No. 2, 1992, pp. 424-432.

[18] Widegren, J.A., Bruno, T.J., "Thermal Decomposition Kinetics of Aviation Turbine Fuel Jet A," *Industrial and Engineering Chemistry Research*, Vol. 47, No. 13, 2008, pp. 4342-4348.

doi: 10.1021/ie8000666

[19] Andersen, P.C., and Bruno, T.J., "Thermal Decomposition Kinetics of RP-1 Rocket Propellant," *Industrial and Engineering Chemistry Research*, Vol. 44, No. 6, 2005, pp. 1670-1676.

doi: 10.1021/ie048958g

[20]   Widegren, J.A., Bruno, T.J., "Thermal Decomposition Kinetics of Kerosene-Based Rocket Propellants. 1. Comparison of RP-1 and RP-2," *Energy & Fuels*, Vol. 23, No. 11, 2009, pp. 5517-5522.

doi: 10.1021/ef900576g

[21]   Widegren, J.A., Bruno, T.J., "Thermal Decomposition Kinetics of Kerosene-Based Rocket Propellants. 2. RP-2 with Three Additives," *Energy & Fuels*, Vol. 23, No. 11, 2009, pp. 5523-5528.

doi: 10.1021/ef900577k

[22]   Coleman, M.M., Selvaraj, L., Sobkowiak, M., and Yoon, E. "Potential Stabilizers for Jet Fuels Subjected to Thermal Stress above 400°C," *Energy & Fuels*, Vol. 6, No. 5, 1992, pp. 535-539.

doi: 10.1021/ef00035a001

[23]   Atria, J.V., and Edwards, T., "High Temperature Cracking and Deposition Behavior of an n-Alkane Mixture," *Symposium on Structure of Jet Fuels IV*, Preprints of the American Chemical Society, Division of Petroleum Chemistry, New Orleans, LA, Vol. 41, 1996, pp. 498-501.

[24]   Corporan, E., and Minus, D.K., "Assessment of Radical Stabilizing Additives for JP-8 Fuel," *34th AIAA/ASME/SAE/ASEE Joint Propulsion Conference*, Cleveland, OH, AIAA Paper 98-3996, July 1998.

[25]   Selvaraj, L., Sobkowiak, M., Song, C., Stallman, J.B., Coleman, M.M., "A Model System for the Study of Additives Designed to Enhance the Stability of Jet Fuels at Temperatures above 400 °C," *Energy & Fuels*, Vol. 8, No. 4, 1994, pp. 839-845.

doi: 10.1021/ef00046a004

[26]   Klingbeil, A.E., Jeffries, J.B., and Hanson, R.K., "Temperature- and Pressure-Dependent Absorption Cross Sections of Gaseous Hydrocarbons at 3.39 μm," *Measurement Science and Technology*, Vol. 17, No. 7, 2006, pp. 1950-1957.

doi: 10.1088/0957-0233/17/7/038

[27]   Klingbeil, A.E., Jeffries, J.B., and Hanson, R.K., "Temperature-dependent mid-IR absorption spectra of gaseous hydrocarbons," *Journal of Quantitative Spectroscopy & Radiative Transfer*, Vol. 107, No. 3, 2007, pp. 407-420.

doi: 10.1016/j.jqsrt.2007.03.004

[28]   Davidson, D.F., Haylett, D.R., Hanson, R.K., "Development of an aerosol shock tube for kinetic studies of low-vapor-pressure fuels," *Combustion and Flame*, Vol. 155, No. 1-2, 2008, pp. 108-117.

doi: 10.1016/j.combustflame.2008.01.006

[29]   Davidson, D.F., Hanson, R.K., "Recent advances in shock tube/laser diagnostic methods for improved chemical kinetics measurements," *Shock Waves*, Vol. 19, No. 4, 2009, pp. 271-283.

doi: 10.1007/s00193-009-0203-0

[30] Haylett, D.R., Davidson, D.F., and Hanson, R.K., "Development of an Aerosol Shock Tube for Kinetic Studies of Low-Vapor-Pressure Fuels," *43rd AIAA/ASME/SAE/ASEE Joint Propulsion Conference*, Cincinnati, OH, AIAA Paper 2007-5678, July 2007.

[31] Haylett, D.R., Lappas, P.P., Davidson, D.F., Hanson, R.K., "Application of an Aerosol Shock Tube to the measurement of diesel ignition delay times," *Proceedings of the Combustion Institute*, Vol. 32, No. 1, 2009, pp. 477-484.

doi:10.1016/j.proci.2008.06.134

[32] Haylett, D.R., Davidson, D.F., Hanson, R.K., "Second-Generation Aerosol Shock Tube: Improved Design," *Shock Waves*, in press.

[33] Haylett, D.R., Cook, R.D., Davidson, D.F., Hanson, R.K., "OH and C_2H_4 species time-histories during hexadecane and diesel ignition behind reflected shock waves," *Proceedings of the Combustion Institute*, in press, available online 6 September 2010.

doi:10.1016/j.proci.2010.05.053

[34] CPIA/M4 Liquid Propellant Manual, The Johns Hopkins University, Chemical Propulsion Information Agency, Columbia, MD, September 1997.

[35] Petersen, E.L., Davidson, D.F., Rohrig, M., Hanson, R.K., "High-pressure shock-tube measurements of ignition delay times in stoichiometric H_2/O_2/Ar mixtures," *Shock Waves – Proceedings of the 20th International Symposium on Shock Waves, Vol. 2*, edited by B. Sturtevant, J.E. Shepherd, and H.G. Hornung, World Scientific, River Edge, NJ, 1996, pp. 941-946.

[36] Petersen, E.L., Davidson, D.F., Hanson, R.K., "Ignition delay times of ram accelerator CH_4/O_2/diluent mixtures," *Journal of Propulsion and Power*, Vol. 15, No. 1, 1999, pp. 82-91.

doi: 10.2514/2.5394

[37] "Detail Specification, Propellant, Rocket Grade Kerosene," MIL-DTL-25576E, 14 April 2006.

[38] "Detail Specification, Turbine Fuel, Low Volatility, JP-7," MIL-DTL-38219D, 21 August 1998.

[39] Huber, M.L., Lemmon, E.W., Ott, L.S., Bruno, T.J., "Preliminary Surrogate Mixture Models for the Thermophysical Properties of Rocket Propellants RP-1 and RP-2," *Energy & Fuels*, Vol. 23, No. 6, 2009, pp. 3083-3088.

doi: 10.1021/ef900216z

[40] Giovanetti, A.J., Spadaccini, L.J., Szetela, E.J., "Deposit Formation and Heat Transfer in Hydrocarbon Rocket Fuels," NASA CR-168277, 1983.

[41] Huber, M.L., Lemmon, E.W., Bruno, T.J., "Effect of RP-1 Compositional Variability on Thermophysical Properties," *Energy & Fuels*, Vol. 23, No. 11, 2009, pp. 5550-5555.

doi: 10.1021/ef900597q

[42] Billingsley, M., Edwards, T., Shafer, L.M., Bruno, T.J., "Extent and Impacts of Hydrocarbon Fuel Compositional Varability for Aerospace Propulsion Systems," *46th AIAA/ASME/SAE/ASEE Joint Propulsion Conference*, Nashville, TN, AIAA Paper 2010-6824, July 2010.

[43] Steele, W.V., Chirico, R.D., Hossenlopp, I.A., Nguyen, A., Smith, N.K., Gammon, B.E., "The thermodynamic properties of 1,2,3,4- and 5,6,7,8-tetrahydroquinolines," *Journal of Chemical Thermodynamics*, Vol. 21, No. 11, 1989, pp. 1121-1149.

doi: doi:10.1016/0021-9614(89)90100-6

[44] Goos, E., Burcat, A., Ruscic, B., "Third Millennium Ideal Gas and Condensed Phase Thermochemical Database for Combustion," available at http://garfield.chem.elte.hu/Burcat/burcat.html, December 2009. Last printed edition was Argonne National Laboratories Report ANL-05/20, Technion Aerospace Report TAE 960, September 2005.

[45] Rebick, C., "Pyrolysis of Heavy Hydrocarbons," In *Pyrolysis: Theory and Industrial Practice*, edited by L.F. Albright, B.L. Cyrnes, and W.H. Corcoran, Academic Press, New York, NY, 1983, pp. 69-87.

[46] Fabuss, B.M., Smith, J.O., Lait, R.I., Borsanyi, A.S., Satterfield, C.N., "Rapid Thermal Cracking of n-Hexadecane at Elevated Pressures," *Industrial and Engineering Chemistry Process Design and Development*, Vol. 1, No. 4, 1962, pp. 293-299.

doi: 10.1021/i260004a011

[47] Fabuss, B.M., Smith, J.O., Lait, R.I., Fabuss, M.A., Satterfield, C.N., "Kinetics of Thermal Cracking of Paraffinic and Naphthenic Fuels at Elevated Pressures," *Industrial and Engineering Chemistry Process Design and Development*, Vol. 3, No. 1, 1964, pp. 33-37.

doi: 10.1021/i260009a009

[48] Edwards, T., "'Kerosene' Fuels for Aerospace Propulsion – Composition and Properties," *38th AIAA/ASME/SAE/ASEE Joint Propulsion Conference*, Indianapolis, IN, AIAA Paper 2002-3874, July 2002.

[49] Davidson, D.F., Oehlschlaeger, M.A., and Hanson, R.K., "Methyl concentration time-histories during iso-octane and n-heptane oxidation and pyrolysis," *Proceeding of the Combustion Institute,* Vol. 31, No. 1, 2007, pp. 321-328.

doi:10.1016/j.proci.2006.07.087

[50] Yu, J, and Eser, S., "Thermal Decomposition of n-Alkanes Under Supercritical Conditions," *Symposium on Structure of Jet Fuels IV*, Preprints of the American Chemical Society, Division of Petroleum Chemistry, New Orleans, LA, Vol. 41, 1996, pp. 488-492.

[51] Vinnitskii, O.M., Rumyantsev, A.N., Musayev, I.A., Sanin, P.I., Lavrovskii, K.P., "Mechanism of Cracking of Higher Paraffins," *Petroleum Chemistry: USSR* (translated from *Neftekhimiya*), Vol. 13, No. 2, 1973, pp. 124-134.

doi:10.1016/0031-6458(73)90007-5

[52] Sirjean, B., Dames, E., Sheen, D.A., You, X.-Q., Sung, C., Holley, A.T., Egolfopoulos, F.N., Wang, H., Vasu, S.S., Davidson, D.F., Hanson, R.K., Bowman, C.T., Kelley, A., Law, C.K., Tsang, W., Cernansky, N.P., Miller, D.L., Violi, A., Lindstedt, R.P., A high-temperature chemical kinetic model of n-alkane oxidation, JetSurF version 1.0, September 15, 2009, (http://melchior.usc.edu/JetSurF1.0).

[53] Violi, A., Yan, S., Eddings, E.G., Granata, S., Faravelli, T., Ranzi, E., "Experimental Formulation and Kinetic Model for JP-8 Surrogate Mixtures," *Combustion Science and Technology*, Vol. 174, No. 11-12, 2002, pp. 399-417.

doi: 10.1080/00102200290021740

[54] Dahm, K.D., Virk, P.S., Bounaceur, R., Battin-Leclerc, F., Marquaire, P.M., Fournet, R., Daniau, E., Bouchez, M., "Experimental and Modeling Investigation of the Thermal Decomposition of n-Dodecane," *Journal of Analytical and Applied Pyrolysis*, Vol. 71, No. 2, 2004, pp. 865-881.

doi:10.1016/j.jaap.2003.11.005

[55] Ranzi, E., Frassoldati, A., Granata, S., Faravelli, T., "Wide-Range Kinetic Modeling Study of the Pyrolysis, Partial Oxidation, and Combustion of Heavy n-Alkanes," *Industrial and Engineering Chemistry Research*, Vol. 44, No. 14, 2005, pp. 5170-5183.

doi: 10.1021/ie049318g

[56] Mawid, M.A., Sekar, B., "Development of a Detailed JP-8/Jet-A Chemical Kinetic Mechanism for High Pressure Conditions in Gas Turbine Combustors," *Proceedings of ASME Turbo Expo 2006: Power for Land, Sea, and Air*, Barcelona, Spain, ASME Paper GT2006-90478, May 2006.

[57] Westbrook, C.K., Pitz, W.J., Herbinet, O., Curran, H.J., Silke, E.J., "A Comprehensive Detailed Chemical Kinetic Reaction Mechanism for Combustion of n-Alkane Hydrocarbons from n-Octane to n-Hexadecane," *Combustion and Flame*, Vol. 156, No. 1, 2009, pp. 181-199.

doi:10.1016/j.combustflame.2008.07.014